Experimental Investigation of Co-flow Effect on Ignition Process of a Methane Jet Diffusion Flame

Qian Wang [a](✉), Jiansheng Yang [b], Yiran Wang [b], Yang Zhang [b], C.Y. Zhao [a]

[a] School of Mechanical Engineering, Shanghai Jiao Tong University, Shanghai, 200240, China

[b] Department of Mechanical Engineering, the University of Sheffield, Sheffield, S1 3JD, UK

1 Introduction

Laminar gas jet diffusion flames have been intensively studied in combustion science [1-6]. Diffusion flames are widely used in industrial systems for safety consideration, since the oxidizer and fuel can be stored separately. In order to improve the stability of diffusion flames, adding co-flow is often considered to be an effective and easy implementation method. Characteristics of diffusion flames in laminar jets have been investigated extensively to understand the stabilization mechanism both for lifted and non-lifted flames.The lift-off characteristics in co-flow jets with highly diluted propane were studied experimentally [7]. The gravity effects on lifted flame oscillation mechanisms have been tackled under co-flow conditions in [8]. A combined computational and experimental investigation that examines the relationship of soot formation and NO in co-flow ethylene air diffusion flames is presented in [9]. The co-flow effect on the interaction between the visible flame and outside vortices of the non-lifted methane diffusion flames has been studied systematically through experimental visualisation methods [10]. It is found that co-flow air can help to create a laminar pattern of the hot gas flow and thus push the initiation point of toroidal vortex to exceed the flame tip; the flame oscillation is then suppressed. However, the aforementioned research mainly focuses on the well-established flame dynamics; the ignition process of diffusion flame with co-flow is rarely studied.

The ignition of a flammable mixture is a fundamental problem in the field of combustion science, which involves complicated chemical reaction and flow variations. Many technological applications requires detailed investigation on the combustion transition from an non-reacting (forced ignition) or a slow reacting state (autoignition) to a fully burning state; for example, the relighting of an aviation gas turbine, the spark-ignition engine and diesel engine, etc. Phuoc et al. [11] investigated the laser spark ignition of a jet diffusion flame experimentally. It is reported that the success of ignition depends on whether the spark initiated reacting gas could undergo a transition from hot plasma to a propagating flame or not. The simulation work by Richardson ES and Mastorakos E. [12] indicates that the ignition can be prohibited by excessive strain rates in a non-premixed flame. The ignition and flame propagation of a methane–air triple flame in a partially premixed jet is investigated experimentally and numerically by Qin et. al.[13]. It is found that during the flame propagation process, the curvature-induced stretch dominates over the hydrodynamic stretch and the flame speed decreases with increasing stretch rate. Zhang and Bray [14] reported that different flame patterns can be formed under

Correspondence to: qianw2006@gmail.com

same flow conditions only by varying the ignition place for the methane diffusion impinging flame. The ignition process of methane and propane diffusion impinging flame was further investigated by Wang and Huang [15,16] through high speed color/schlieren and image processing techniques. It is found that the ignition process is sensitive to plate-to-nozzle height, fuel flow rate, ignition position and fuel type. However, the co-flow air effect on the ignition process of methane diffusion flame is still not reported to the best knowledge of the authors.

The availability of modern colour high-speed camera not only is able to visualise the behaviours of time-dependent flame structure evolution but also provides useful information on the flame colour change. For hydrocarbon flames, the visible emanating energy can be attributed to the spectra of electronically excited combustion radicals CH* (430 nm), C_2* (C_2* Swan system, dominant emissive band head at 473.71 nm and 516.52 nm), and the continuous spectrum from solid carbon/soot [17]. The intensity of the energy released by these spectra is related to a number of factors such as burning condition, fuel composition and fuel-to-oxidizer ratio, which would consequently affect the colour perceived from a given flame. Thus, the colour of a flame can be used to provide information on its general spectrometric composition. Modern digital high-speed colour cameras, unlike its more commonly employed monochronmatic counterpart, encodes the captured visible radiation into three discrete signal ranges with sensitively peaking in the R, G and B portion of the visible electromagnetic spectrum. In this form, digital colour cameras can be considered as a device that offers limited multi-spectral discrimination in addition to its designed spatial functionality. The blue and green emissions (in the RGB colour space) were found to model well the CH* and C2* chemiluminescence intensities, respectively. Based on this, a Digital Flame Colour Discrimination (DFCD) combustion quantification scheme has been established by Huang [18]. In DFCD method, the appropriate use of colour signals identified from the different flame radiation induction regime is able to provide useful correlations such as indicating the trends of spectroscopic-derived CH* and C2* emission distributions over range of equivalence ratios [19], and the local fuel/air mixture [16]. It also has demonstrated useful application in identifying the concurrent existence of weak chemiluminescence induced kernel volumes that along with the dominant soot continuum-radiation during the ignition of non-premixed hydrocarbon flames in both the laboratory Bunsen burner [19] and the Rolls-Royce sub atmospheric relight test rig ignition sequences [20]. In this study, the ignition process of a methane diffusion flame under different co-flow air velocities have been investigated experimentally using high speed color and schlieren imaging techniques. DFCD method has been applied to reveal otherwise difficult to visualise flame initiation process, while the hot gas evolution outside the visible flame has been investigated via schlieren imaging. The results have provided improved phenomenological insight into the nature of ignition process and should provide physical insights for modeling studies.

2 Experimental setup

The schematic setup of the experimental system is shown in Fig. 1. In the experiments, methane was used as fuel. The air and fuel was controlled by mass flow controllers. The fuel jet was surrounded by a coaxial air jet. The fuel was injected through a central nozzle of 4.57 mm in diameter. The co-flow air nozzle has a diameter of 37.8 mm. The air was straightened by a fine meshed honeycomb inside the air nozzle. The detail structure of the burner can be referred to [10]. A Z-type schlieren imaging system was used to investigate the flow dynamics and structures. The schlieren system consists of a LED lamp as the light source and two parabolic mirrors with 0.3048 m (12 in.) in diameter and 3.048 m (10 feet) in focal length. The images were recorded by a high speed camera (Photron FASTCAM SA4) with a resolution of 1024 by 1024 pixels. Table 1 shows the test conditions of the experiments. The fuel flow rate was fixed at 0.182 l/min, while the co-flow air flow rate was ranging from 5 l/min to 175 l/min. The velocity ratio between air and fuel varies in a wide range from 0.36 to 12.5. Electric spark from a Kawasaki ignition-coil (TEC-KP02) was generated between a pair of steel electrodes with sharpened edges to reduce the heat loss. The electric charge to the coil was delivered from a sealed lead acid battery (12 volt, 1.2 Ah) to produce a consistent spark voltage of approximately 1 kV.

The ignition electrodes were placed at a distance of 14 mm downstream of the burner nozzle exit with a spark gap of 9 mm.

Table 1. Test conditions

Gas type	Volume flow rate (l/min)	Velocity (m/s)	Re No.	V_a/V_f [a]
Methane (CH_4)	0.182	0.216	55.4	/
Air	5	0.077	171	0.36
Air	14	0.216	479	1.00
Air	25	0.385	855	1.78
Air	50	0.772	1710	3.56
Air	75	1.155	2565	5.34
Air	100	1.540	3420	7.13
Air	125	1.925	4275	8.91
Air	150	2.310	5130	10.7
Air	175	2.695	5985	12.5

[a] V_a: co-flow air velocity; V_f: fuel velocity

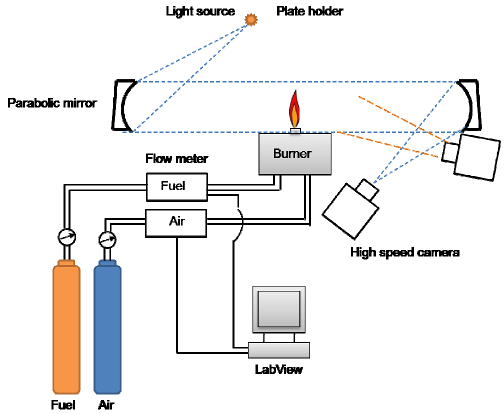

Figure 1. Schematic of the experimental setup

3 Results and discussions

The cold fuel flow pattern can be visualised through high speed schlieren imaging before ignition. Three different patterns can be observed and have been shown in Fig.2: a laminar fuel jet at 5 l/min, 14 l/min and 25 l/min; regular vortex shedding structure at 50 l/min and 75 l/min; more turbulent and finer structures are observed at 100 l/min and higher air flow rates. The dramatic differences have shown that the fuel/air mixing is enhanced with the increasing of co-flow air flow rates, which might have great effect on the ignition process following.

The ignition process has been investigated by high speed color and schlieren imaging respectively. The repeatability of the experiments was verified by measuring the hot gas movement on the schlieren images. The ignition process has been repeated for 10 times of the cases 5 l/min, 14 l/min and 50 l/min. The mean relative tolerance based on the flame propagation measurement is less than 5%, which indicates that the experiments are reasonably repeatable. In order to show the invisible weak blue flame during the ignition process, DFCD method was applied to process the original color image. By setting filters within HSV model space, the diffusion flame like yellowish and premixed flame like bluish flame colorations can be identified and separated. Then the identified blue color pixels were selectively enhanced by 35 times in the RGB model space to make the very weak blue flame observable. The comparison between the original and blue color-enhanced images is shown in Fig. 3. It can be seen that the blue color flame can hardly be observed on the original high speed image at a shutter speed of 1/500 s; but can be visualised clearly on the enhanced image. The results demonstrate that it can be quite misleading in interpretation of high speed or high shutter speed flame colour images without careful digital enhancement because the blue flames are so much weaker than the yellowish diffusion flame and it can be completely masked.

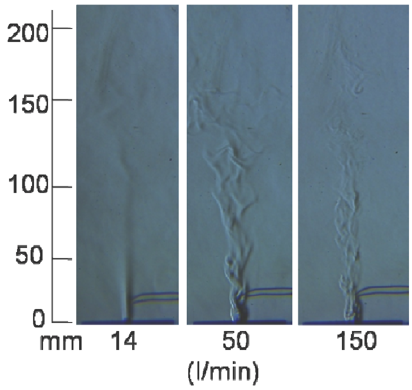

Figure 2. Typical tested cold fuel flow patterns

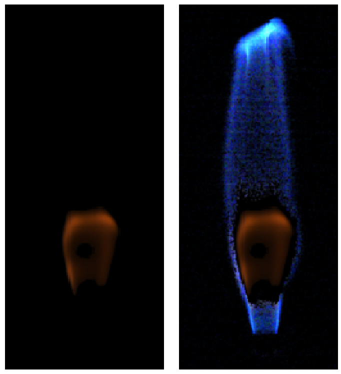

Figure 3. Comparison between the original and the blue color-enhanced images

Figure 4 and 5 shows the blue color-enhenced and schlieren image sequences of the ignition process at 5 l/min, 50 l/min and 100 l/min respectively. Although the schlieren and direct imaging sequences were not recorded at the same time, the good repeatability of the experiments can still enable an appropriate comparison between them. The spark initiation time can be recognised from the high speed imaging sequences. It is worth pointing out that the hot gas volume generated by flame is much larger and higher than the visible flame. Thus the physical scale of the schlieren and direct color imaging is very different. It can be seen from the color images that, at the very beginning of the ignition, irregular blue flame kernels are formed with clear curved boundaries. Then the flame propagates along the fuel/air mixing boundaries: forming a circle in jet radial direction, growing longer in jet axial direction, and the lower flame boundary attaching the nozzle exit gradually. At low air flow rates (5 l/min, 14 l/min, 25 l/min and 50 l/min), a hollow blue flame with a brighter tip is formed at first, due to the fuel and air mixing along the fuel jet boundary. The inner zone is filled with fuel rich mixtures and heated by the surrounding blue flame. The fuel rich mixtures begin to decompose under high temperatures and a yellow-reddish flame can be observed after about 50 ms, indicating high volume concentration of soot particles. It is also interesting to note that the formation of the sooty flame is observed at a similar time after ignition in the three cases. The diffusion flame changes color from dark red to bright yellow, which indicates the flame temperature is increasing dramatically because of the further reaction with air. At 50 l/min, a Bunsen like flame shape formed near the burner nozzle. The upper part of the flame is shedding gradually by buoyancy effects, after which a steady diffusion flame can be formed without oscillating finally. The flame oscillating is suppressed by the co-flow air as reported in [10]. When the air flow rates are higher than 75 l/min, the yellow-reddish flame is not observable. This may be due to the enhanced mixing between fuel and air because of the large velocity gradient effect. In all the cases, the flame height is increasing with time at first as a result of the excessive fuel accumulated before ignition. The flame height starts to decay when the excessive fuel is consumed and finally reaches a steady state with a constant flame height. Moreover, with the increasing co-flow air velocities, the flame height at steady state becomes shorter, which means the same amount of fuel is burnt at smaller regions. That is to say, the burning velocity of the mixture must be increased due to the enhanced fuel/air mixing. As a result, the time from ignition to steady flame establishment is shorter at higher co-flow air velocities.

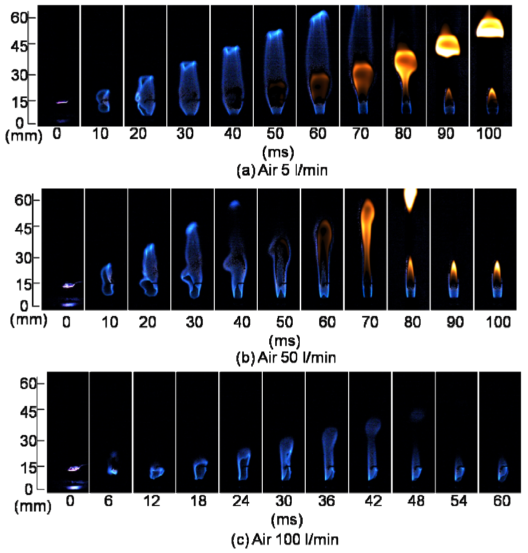

Figure 4. Blue-color DFCD enhanced imaging sequences

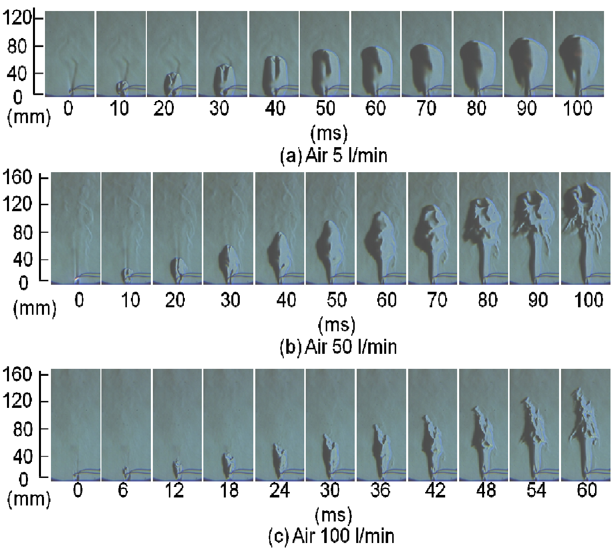

Figure 5. Schlieren imaging sequences

The hot gas evolution at the initial stage of ignition can be observed from the high speed schlieren images. Two typical structures can be recognised: a hot gas bulge at upper part due to the excessive fuel accumulation and a laminar central jet developed from nozzle exit even the corresponding cold jet is turbulent as indicated in Fig. 2. The tip and bottom positions of the bulge shown in Fig.6a were tracked at different ignition cases, as plotted in Fig. 6b and 6c respectively. The mean velocities of the tip and bottom of the bulge have been estimated and are shown in Fig. 6d. It can be seen that with the increasing of air flow rates, both the tip and bottom bulge velocity increase accordingly but not in a linear form, which is a result of both the buoyancy and co-flow effect.

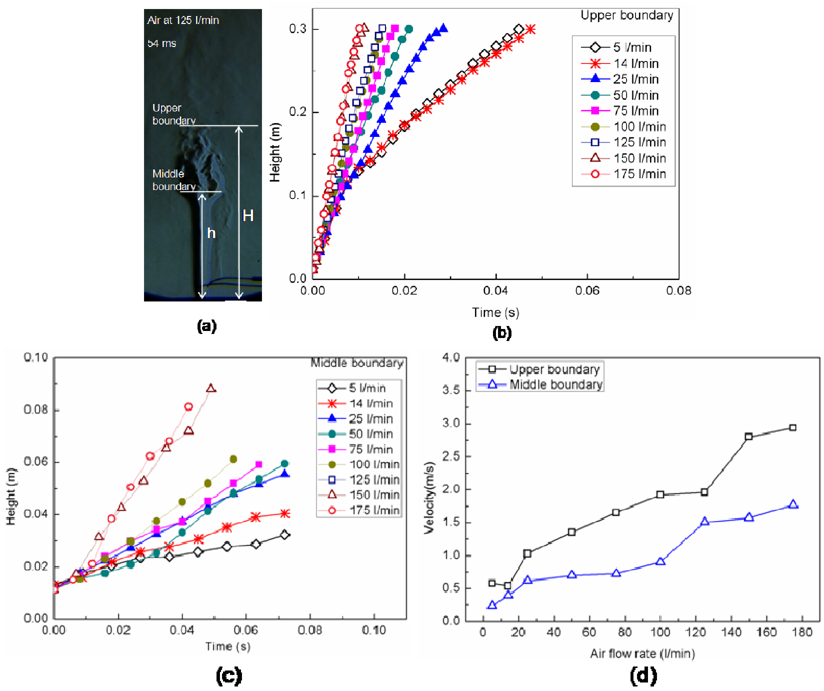

Figure 6. (a) Illustration of the tip and bottom positions; (b) the tip position tracing with time; (c) bottom position tracing with time; (d) tip and bottom moving velocity at different air flow rates

4. Conclusions

The co-flow effect on the ignition process of laminar methane diffusion flames have been investigated using high speed schlieren and color imaging techniques. The burner exit velocity ratio based on the cold co-flow air and fuel is tested in a wide range from 0.36 to 12.5, which corresponds to laminar flow regime at lower ratios and turbulent one at higher ratios. By enhancing the weak blue flame selectively, the ignition process is visualized correctly through the enhanced high speed color imaging sequences. It is observed that the yellowish diffusion flame is formed first inside the hollow blue flame pocket at co-flow air flow rates no more than 50 l/min, while only blue flame can be observed at high air flow rates. Both the flame height and the time from ignition initiation to steady flame establishment is decreasing with the increasing of co-flow air velocity, which is due to the increased burning velocity with enhanced fuel/air mixing. The penetrating process of the hot gas generated by flame has been visualized by high speed schlieren images. A hot gas bulge is formed due to the fuel accumulation before ignition. A laminar pattern can be observed from the nozzle exit due to the strong upward co-flow air momentum coupled with combustion. It is found that both the hot gas bulge and laminar pattern move faster at higher co-flow air velocities. The nonlinear increasing trend may be due to the complex interactions among the hot gas buoyancy, the burning velocity, the velocity gradient between the co-flow air and hot gas, etc.

References

[1] D.S. Chamberlin, A. Rose, Proc. Combust. Inst.1–2 (1948) 27–32.
[2] L.D. Chen, J.P. Seaba, W.M. Roquemore, L.P. Goss, Proc. Combust. Inst. 22 (1989) 677–684.
[3] T.Y. Toong, F.S. Richard, M.S. John, Y.A. Griffin, Proc. Combust. Inst. 10 (1965) 1301–1313.
[4] V.R. Katta, W.M. Roquemore, Combust. Flame 92 (1993) 274–282.
[5] I. Kimura, Proc. Combust. Inst. 10 (1965) 1295–1300.
[6] J. Buckmaster, N. Peters, Proc. Combust. Inst. 21 (1988) 1829–1836.
[7] S. H. Won, S.H. Chung, M.S. Cha, B.J. Lee, Proc. Combust. Inst. 28 (2000) 2093–2099.
[8] S.H. Won, J. Kim, M.K. Shin, S.H. Chung, O. Fujita, T. Mori, J.H. Choi, K. Ito, Proc. Combust. Inst. 29 (2002) 37–44.
[9] B.C. Connelly, M.B. Long, M.D. Smooke, R.J. Hall, M.B. Colket, Proc. Combust. Inst. 32 (2009) 777–784.
[10] Q. Wang, H. Gohari Darabkhani, L. Chen, Y. Zhang, Exp. Therm. Fluid Sci. 37 (2012) 84–90.
[11] Phuoc TX, White CM, McNeill DH, Opt. Laser. Eng. 38 (2002) 217–32.
[12] Richardson ES, Mastorakos E, Combust. Sci. Technol. 179 (2007) 21–37.
[13] Qin X, Choi CW, Mukhopadhyay A, Puri IK, Aggarwal SK, Katta VR, Combust. Theor. Model. 8 (2004) 293–314.
[14] Zhang Y, Bray KNC, Combust. Flame 116 (1999) 671–674.
[15] Q. Wang, H.W. Huang, Y. Zhang, Fuel 108 (2013) 177-183
[16] Huang HW, Yang J, Wang Q and Zhang Y, Fuel 103 (2013) 334-346
[17] Gaydon AG, The Spectroscopy of Flames, Chapman and Hall, Harlow, London, 1974.
[18] Huang HW and Zhang Y, Meas. Sci. Technol. 19 (2008) 085406.
[19] Huang HW and Zhang Y, Fuel 90 (2010) 48-53.
[20] Huang HW and Zhang Y. Meas. Sci. Technol. 22 (2011) 075401.